Role of resonance radiation trapping in the mechanisms of constriction of the glow discharge. Theory and experiment.

IOP Conf. Series: Journal of Physics: Conf. Series **1038** (2018) 012126 doi:10.1088/1742-6596/1038/1/012126

Role of resonance radiation trapping in the mechanisms of constriction of the glow discharge. Theory and experiment.

Yu B Golubovskii[1], A V Siasko[1], D V Kalanov[1] and V O Nekuchaev[2]

[1]Faculty of Physics, St Petersburg State University, Ulianovskaia ul. 3, St Petersburg 198504, Russian Federation

[2]Ukhta State Technical University, Pervomaiskaia ul. 13, Ukhta 169300, Russian Federation

E-mail: aleksei.siasko@gmail.com, y.golubovskiy@spbu.ru

Abstract. The paper presents latest results of constricted glow discharge simulations. Detailed self-consistent plasma model includes a large set of plasma chemical reactions, considering inhomogeneous gas heating and accurate solution of radiation transport equation. Results of the computer simulations were compared with an experimental data of positive column constriction in neon and argon. Experimental plasma diagnostics was performed using classic methods of emission and absorption spectroscopy and a line ratios method. Comparison of the obtained results allows to reveal the influence of resonance radiation trapping on the plasma parameters of a constricted discharge.

1. Introduction

Constriction is an interesting phenomenon in gas discharges which is observed as an abrupt compression of plasma to a thin bright cord on the discharge axis when pressure and current reach the critical values. This phenomenon has been studied in detail both theoretically and experimentally [1–6]. However, the problem of radiation trapping was ignored in these works so far as the Holstein effective lifetime approximation (escape-factor approximation) was used, which assumes that excitation and destruction of resonant atoms are local. Radiation transport leads to a spatial redistribution not only of resonant atoms but also metastable atoms and other plasma components related to the resonant atoms through the collisional - radiative processes. It is of great interest to reveal the influence of radiation trapping in the mechanism of constriction. Constricted discharge is quite a convenient object for the analysis since in diffuse state at low currents spatial distributions of plasma components are close to the fundamental modes and traditional description in terms of effective diffusion and radiation lifetimes is applicable. But when the plasma contracts to a thin cord higher radiation and diffusion modes start playing a crucial role [7]. First attempt of correct account of radiation trapping in the mechanism of constriction was made in paper the [8] using a simple discharge model.

Current work presents a detailed model of a constricted glow discharge with a large set of plasma chemical reactions, including accurate solution of kinetic equation and account of inhomogeneous gas heating. The model allows one to compare traditional approach of the Holstein escape factor with a precise treatment of the resonance radiation. The role of radiation trapping is demonstrated on a formation of radial profiles of various plasma components and current-voltage

characteristics.
Along with simulations, experimental study of positive column constriction in neon and argon was performed. In particular, field-current characteristics in neon and argon, densities and radial profiles of the excited states $2p^5 3s$ and $2p^5 3p$ in neon and $3p^5 4s$ and $3p^5 4p$ in argon (1s and 2p in Pashen's notation) were measured. Densities and radial profiles were obtained using classic methods of emission and absorption spectroscopy [9] as well as the line ratios method [10]. Similar features and differences in the mechanisms of discharge constriction in neon and argon are discussed. Obtained results show good agreement with simulations.

2. Self-consistent glow discharge model

A detailed model of the glow discharge presented in this paper is similar to a model of argon discharge described in [11]. The model allows to treat the resonance radiation transport accurately and makes it possible to obtain a continuous hysteresis in transition between diffuse and constricted regimes.
All elementary processes, included in the model of neon, are listed in table I with the references.

Table 1. Plasma-chemical reactions included in the collisional-radiative model.

Process	Notation	Ref. (Neon)
Elastic scattering	$Ne + e \rightarrow Ne + e$	[12]
Excitation	$Ne + e \rightarrow Ne^*(1s, 2p) + e$	[13]
Intermixing	$Ne^* + e \rightarrow Ne^* + e$	[14]
Direct ionization	$Ne + e \rightarrow Ne^+ + 2e$	[12]
Stepwise ionization	$Ne^* + e \rightarrow Ne^+ + 2e$	[12]
Chemoionization	$Ne^* + Ne^* \rightarrow Ne_2^+ + e$	[15]
Ion conversion	$Ne^+ + 2Ne \rightarrow Ne_2^+ + Ne$	[16]
Dissociative recombination	$Ne_2^+ + e \rightarrow Ne^* + Ne$	[17]
Dissociation	$Ne_2^+ + e \rightarrow Ne^+ + Ne + e$	[18]
Excimer formation	$Ne^* + 2Ne \rightarrow Ne_2^* + Ne$	[19]
Resonance radiation	$Ne^*(1s_2, 1s_4) \rightarrow Ne + h\nu$	[20]
Excimer radiation	$Ne_2^*(^3\Sigma_u) \rightarrow 2Ne + h\nu$	[21]
Visible radiation	$Ne^{**} \rightarrow Ne^* + h\nu$	[22]
Metastable diffusion	$Ne^* \rightarrow$ wall	[23]

Most of the rate constants of processes with electrons were calculated by an averaging of the cross sections over the electron energy distribution function (EEDF). The EEDF is obtained by solving the Boltzmann equation. Densities and radial profiles of plasma components were found from the balance equations. Resonant atoms are described by an integral equation of resonance radiation transport while all other plasma components are described by the diffusion equation. Papers [8, 11] give a detailed description of applied balance equations and a thermal balance equation describing gas heating which affects the filament radius. The applicability limits of the model and solution algorithm are also discussed in detailsin mentioned papers.

3. Experimental plasma diagnostics

3.1. Experimental set-up

The experiment was conducted with the argon and neon cylindrical discharge tubes. The neon-filled tube with horizontal orientation had a radius of 1.5 cm, pressure p =60 Torr and a length

between the electrodes $d = 70$ cm. The argon tube was oriented vertically and spectrally pure argon was fed through the vacuum system with liquid-nitrogen cooled traps. The radius of the tube was 2.3 cm, pressure p =42 Torr and a length between the electrodes $d = 50$ cm. Electrical characteristics of DC glow discharges were studied in a range of currents 5 - 70 mA/cm.
To perform spatial absorption measurements, a second tube with ICP discharge in 2 Torr argon or neon (depending on the main source) was placed behind the main source. A back window of the source tube was uniformly illuminated with a lens. A registration system consisted of a monochromator Acton SpectraPro 2300i with a high-speed camera pco.1200hs. Radial scanning was performed with the high-speed camera, so an instrumental function of the experimental set-up was determined by a pixel size of the camera. Scheme of the experimental set-up with fragments of constricted neon and argon discharges are presented in figure 1.
Both constricted discharges represented a thin plasma cord located at the axis of a discharge.

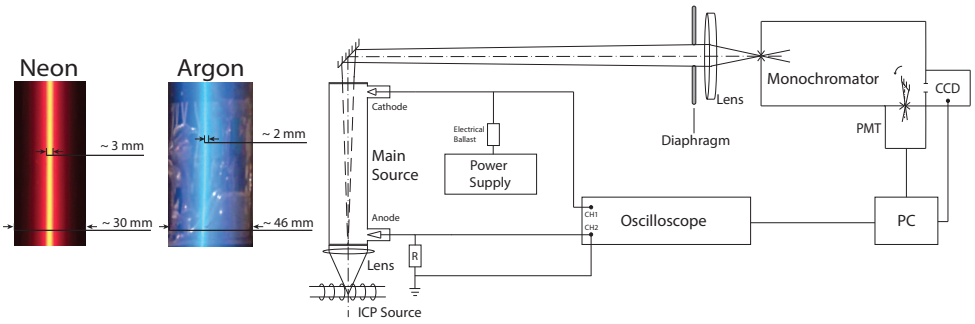

Figure 1. Scheme of the experimental set-up with the fragments of constricted neon and argon discharges.

Reduced diameter of a filament in neon $(d/R)_{Ne} \approx 0.1$ is much bigger than in argon $(d/R)_{Ar} \approx 0.04$. Spatial distribution of a luminous cord determines the excitation and ionization zones in the constricted discharges. The discharges are surrounded with a weak glow which is continuum spectrum of electrons deceleration by neutral species. The intensity of the glow is related to the electron density and electron temperature.
Densities and radial profiles of the $1s$ and $2p$ states in argon and neon were obtained using conventional emission and absorption spectroscopy technique [9] and a relatively new line ratios method [10]. Application of the classic emission and absorption spectroscopy method is described in details in [11] so only a theory of line ratios method will be discussed below.

3.2. Line ratios method

One of the method that was implemented to measure radial profiles and densities of lower excited $1s$ states was a line ratios method which is based on obtaining a set of algebraic equations from photon flux ratios for lines radiating from same upper state to different lower states. For a specific transition $i \to j$ a photon flux that is projected onto the entrance slit of the spectral device will be written as:

$$\Phi_{ij} \propto N_i A_{ij} h\nu_{ij} L S(k_0 L), \tag{1}$$

where N_i is a density of radiating atoms, A_{ij}- transition probability, $h\nu_{ij}$- energy of quant and $S(k_0 L)$ is a Ladenburg function which takes into account the reabsorption of the photons along the plasma source. Thus, a ratio of the photon fluxes from the same upper level i to different lower levels j and k will be

$$\frac{\Phi_{ij}}{\Phi_{ik}} = \frac{A_{ij}\nu_{ij} S\left(K_{0j} L\right)}{A_{ik}\nu_{ik} S\left(K_{0k} L\right)} \tag{2}$$

The Ladenburg function can be represented as a function of the lower state density

$$S(k_0 L) = S(a_{ij} N_j),$$

$$a_{ij} = \frac{\lambda_{ij}^2 g_i}{8\pi g_j} A_{ij} \varepsilon_0 L, \qquad \varepsilon_0 = \frac{2\sqrt{ln2}}{\pi^{3/2}} \frac{a}{\Delta\nu_D} \int_{-\infty}^{\infty} \frac{exp(-y^2)dy}{a^2 + y^2}.$$

ε_0 is an emission coefficient in the center of a spectral line assuming Voigt lineshape, g_i and g_j are statistical weights, λ_{ij}- central wavelength of the transition and parameter $a = \sqrt{ln2}\Delta\nu_L/\Delta\nu_D$ characterizes the ratio of a Lorentz half-width to a Doppler half-width. Using equation (12) the densities of lower-lying states can be determined. A system of homogeneous non-linear equations will have a form

$$S(a_{ij} N_j) - \frac{\Phi_{ij} A_{ik} \nu_{ik}}{\Phi_{ik} A_{ij} \nu_{ij}} S(a_{ik} N_k) = 0.$$

Ratio of the photon fluxes Φ_{ij}/Φ_{ik} is a measured value. Representing the Ladenburg function in the form of series expansion one can solve the equation system using the least-squares method. An increase of the number of equations will enhance the accuracy of the method.

4. Results

Figure 2 contains volt-ampere characteristics measured in the neon and argon discharges under described conditions compared to the simulations carried out in case of traditional effective lifetime approximation and precise treatment of resonance radiation transport. Electric field in

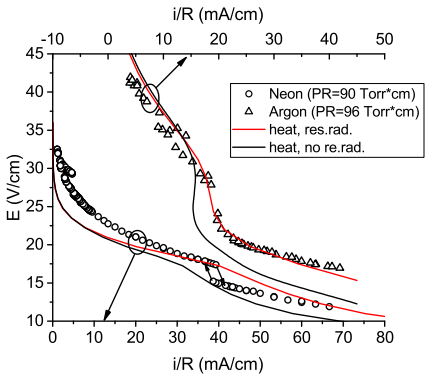

Figure 2. Measured electric field in argon (△) and neon (○) with corresponding numerical results: ignoring radiation transport (black lines), account of radiation transport (red lines).

argon is much larger than in neon. Even though the ionization potential in argon is lower than in neon, difference in cross-sections of electron - atom elastic collisions, which is much larger in argon, leads to a depletion of fast electrons in the EEDF in case of argon. Lack of fast electrons causes a decrease of ionization frequency. To maintain the balance of ionization with diffusion electric field in argon increases.

In measured electric fields diffuse states switch to constricted ones with abrupt changes of discharge voltage when the current exceeds a critical value - about 40 mA/cm for neon and 10 mA/cm for argon. In neon transition from the diffuse to the constricted state and in the opposite direction is accompanied by a perceptible hysteresis.

In the simulations, precise account of radiation transport resulted in a shift of critical currents towards higher values so the electric field increases in the constricted states. Gas heating which was taken into account led to a smoothing of the characteristics near the critical currents so no hysteresis is observed.

Figure 3 shows absolute densities of $1s$ states in argon (a) at $i = 40$ mA and in neon (b) at $i = 70$ mA. For the neon discharge, absolute densities were obtained using classic absorption method

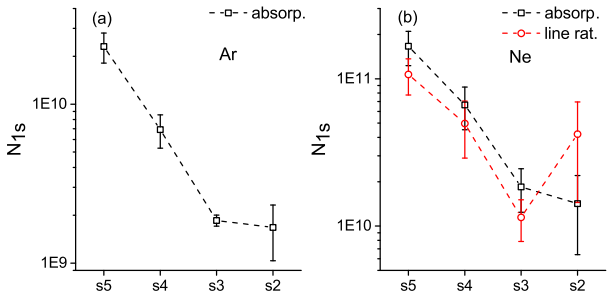

Figure 3. Absolute densities in argon (a) and neon (b) measured using classic method of emission and absorption spectroscopy (black lines) and line ratios method (red line).

and the line ratios method. As it can be seen both methods give identical densities within the measuring and statistical error except for the higher $1s2$ level, where the intensity of the lines is very weak that cause big errors. Densities in neon are higher on the order of magnitude than in argon.

Radial profiles of higher $2p$ states, which are presented in figure 4 for constricted discharges at

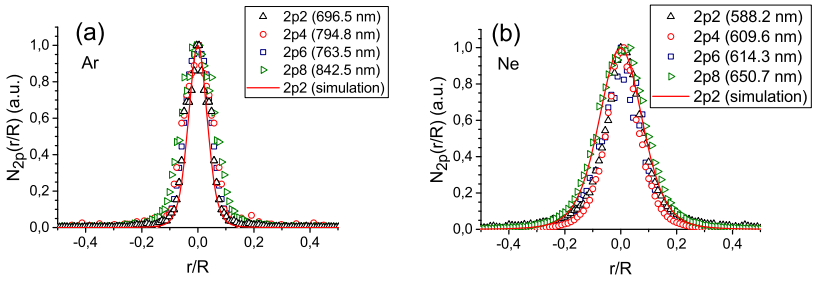

Figure 4. Normalized radial profiles of $2p-$states in argon (a) and neon (b) over different wavelengths with simulations results.

40 mA in argon and 70 mA in neon over different wavelengths are more narrow in argon. As in volt-current characteristics, observed difference is caused by a distinction of elastic electron - atom scattering cross sections. Higher cross section in argon leads to a bigger ionization rate which means that the radial profile in argon should be more constricted than in neon to maintain the balance of ionization, diffusion and recombination at high current.

Red lines in figure 4 represent the result of simulations for $2p_2$ state radial profile, which are

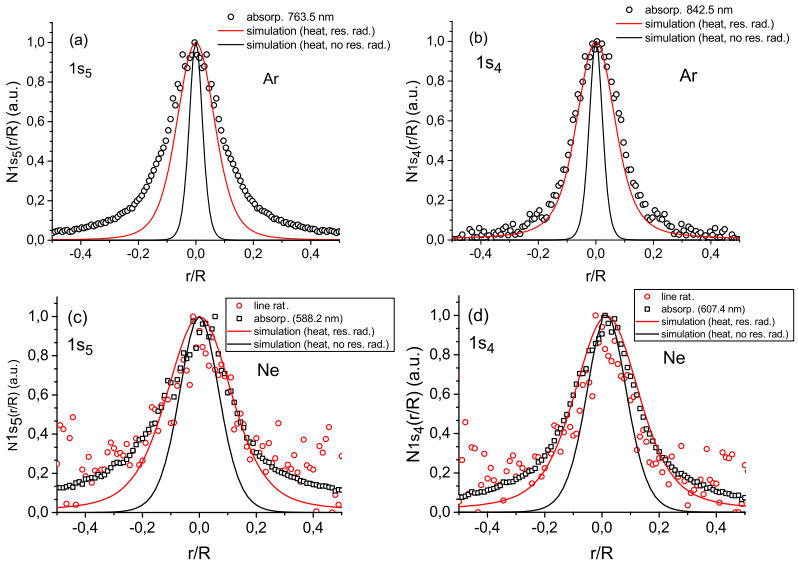

Figure 5. Normalized radial profiles of $1s_5$ and $1s_4$ states in argon (a, b) and neon (c, d) obtained from classic absorption method and line ratios method with theoretical simulations.

in good correlation with the experimental results.

Figure 5 shows radial profiles of metastable $1s5$ and resonant $1s4$ states in argon (a, b) and neon (c, d) discharges. As before, radial profiles in argon are more narrow than in neon. For both discharges black lines correspond to the simulations in the approximation of the effective lifetime ignoring redistribution of resonant atoms due to resonance radiation trapping. When the resonance radiation transport is taken into account precisely (red lines), radial profiles become broadened. It is caused by the emergence of resonant atoms outside the excitation zone due to a reabsorption of the photons. The correct account of radiation transport gives better correlation to the experimental results.
Radial profiles in neon were measured using classic absorption method and the line ratios method. As it can be seen in the central part of the discharge both methods give identical results. However, moving to the outer region, the error of the line ratios method grows rapidly. It can be explained by a higher sensitivity of the line ratios method to the light intensity which is very low far from the discharge center in the constricted discharge.

5. Conclusion

Detailed self-consistent model which allows simulating constricted glow discharge using traditional approximation of Holstein effective lifetime and accurate treatment of radiation transport was applied to argon and neon noble gases. In constricted discharges, precise consideration of radiation transport leads to a broadening of radial profiles of plasma components, decrease of absolute densities at the discharge axis as a result of radial redistribution and a shift of a constriction current on the volt-ampere characteristics towards higher values.
Demonstrated radial profiles in argon discharge were obtained to be more narrow than in neon and the reasons of this phenomena were discussed as well as the difference in volt-ampere characteristics.
Experimental diagnostics performed with classic absorption method and line ration method show good correlation between the results. But the error given by the line ratios method becomes very high when the light intensity is insufficient.

6. References

[1] Petrov G M and Ferrerira C M 1999 *Phys. Rev.* **59** 3571
[2] Ionikh Y Z, Meshchanov A V, Petrov F B, Dyatko N A and Napartovich A P 2008 *Plasma Phys. Rep.* **34** 867
[3] Dyatko N A, Ionikh Y Z, Kochetov I V, Marinov D L *et al.* 2008 *J. Phys. D: Appl. Phys.* **41** 055204
[4] Shkurenkov I A, Mankelevich Y A and Rakhimova T V 2008 *Plasma Phys. Rep.* **34** 780
[5] Shkurenkov I A, Mankelevich Y A and Rakhimova T V 2009 *Phys. Rev. E* **79** 046406
[6] Gnybyda M, Loffhagen D and Uhrlandt D 2009 *IEEE Trans. Plasma Sci.* **37** 1208
[7] Golubovskii Y B, Siasko A V and Nekuchaev V O 2017 *Plasma Sources Sci. Technol.* **26** 015012
[8] Golubovskii Y B and Mayorov V A 2015 *Plasma Sources Sci. Technol.* **24** 025027
[9] Loureiro J and Amorim J 2016 *Kinetics and spectroscopy of low temperature plasmas* (Springer Int. Publ.)
[10] Schulze M, Yanguas-Gil A, Keudell A and Awakowicz P 2008 *J. Phys. D: Appl. Phys.* **41** 06520
[11] Golubovskii Y, Kalanov D and Maiorov V 2017 *Phys. Rev. E* **96** 023206
[12] Zatsarinny O and Bartschat K 2012 *Phys. Rev. A* **85** 062710
[13] Zatsarinny O and Bartschat K 2012 *Phys. Rev. A* **86** 022717
[14] Dyatko N A, Latyshev F E, Mel'nikov A S and Napartovich A P 2006 *Plasma Physics Reports* **32** 158
[15] Sheverev N A, Stepaniuk V P and Lister G G 2002 *Journal of Applied Physics* **92** 3453
[16] Hackman R 1966 *British Journal of Applied Physics* **17** 197
[17] Frommhold L, Biondi M A and Mehr F J 1968 *Phys. Rev.* **165** 44
[18] Marchenko V S 1983 *Zh. Eksp. Teor. Fiz.* **85** 500
[19] Virin L I, Dzhatspanyan R V, Karachevtsev G V, Potapov V K and Tal'rose V L 1979 *Ion-molecule reactions in gases* (Moscow: Nauka)
[20] Fuhr J A and Wiese W L 1998 *CRC Handbook of Chemistry and Physics* (Boca Raton, Fl: CRC Press)
[21] McCusker M 1984 *The rare gas excimers* (Berlin, Heidelberg: Springer Berlin Heidelberg) p 47
[22] Krebs K 1936 *Z. Phys.* **101** 604
[23] Phelps A V and Molnar J P 1953 *Phys. Rev.* **89** 1202